

# Stochastic Control of Sensitive Nonlinear Motions of an Ocean Mooring System

**Paul E. King**

Program Leader  
U.S. Department of Energy,  
Albany Research Center,  
Albany, OR 97321

**Solomon C. Yim**

Professor  
Coastal and Ocean Engineering Program,  
Department of Civil and Construction  
Engineering,  
Oregon State University,  
Corvallis, OR 97331  
e-mail: solomon.yim@oregonstate.edu

*Complex sensitive motions have been observed in ocean mooring systems consisting of nonlinear mooring geometries. These physical systems can be modeled as a system of first-order nonlinear ordinary differential equations, taking into account geometric nonlinearities in the restoring force, quadratic viscous drag, and harmonic excitation. This study examines the controllability of these systems utilizing an embedded approach to noise filtering and online controllers. The system is controlled using small perturbations about a selected unstable cycle and control is instigated for periodic cycles of varying periodicities. The controller, when applied to the system with additive random noise in the excitation, has marginal success. However, the addition of an iterated Kalman filter applied to the system increases the regime under which the controller behaves under the influence of noise. Because the Kalman filter is applied about locally linear trajectories, the feedback of the nonlinearities through the filter has little effect on the overall filtering system. [DOI: 10.1115/1.2428323]*

*Keywords: nonlinear, stochastic, mooring system, control, iterated Kalman filter*

## Introduction

Sensitive nonlinear responses, including chaotic motions, have been predicted in a mass moored in a fluid medium subject to wave excitations and which is characterized by a large geometric nonlinearity in the restoring force and viscous drag excitation. These systems include sonars, remote sensors, and data collection devices deployed in the ocean environment and which are of interest to the U. S. Navy and the U. S. Department of Energy. This class of fluid–structure interaction problems contains highly nonlinear drag and mooring effects. The overall effects of the nonlinear fluid loads on the structure can be approximated in terms of an added inertia and a nonlinear coupling of the Morison form [1,2]. The nonlinear mooring resistance force can be approximated by a low-order polynomial and hence the resulting mathematical models of these systems are reducible to a low degree system of ordinary differential equations. This order of approximation is often acceptable for preliminary analysis and design of the types of fluid–structure systems considered.

Preliminary analysis of experimental data from such a system as modeled here has demonstrated the likely presence of sensitive and chaotic motions in noisy environments [3]. These sensitive motions are not considered in the fluid–structure system design. Should the unpredictability of the sensitive behavior observed in these systems be deemed undesirable, methods of analyzing the system response to harmonic and noisy excitations and subsequent control of the systems are needed. By representing the desirable states of motion of the nonlinear response of the system with unstable periodic orbits (UPOs), a consistent means of characterizing the strange attractors can be obtained [4]. Thus, the system can be characterized by such topological invariants as the entropy or the Lyapunov spectrum [5]. The analysis and control procedure presented in this study utilizes this representation of the sensitive response to its advantage.

Figure 1 is a schematic of a system moored by cables in a fluid medium. The fluid itself is undergoing motion and an associated

excitation force is induced which can be described by a forcing function of the form  $F(\ddot{x}, \dot{x}, t)$  where  $\dot{x} = dx/dt$  and  $\ddot{x} = d\dot{x}/dt$ . With restraints for vertical and rotational motion, this system is modeled as a single-degree-of-freedom (SDOF) system for the surge,  $x$  [1]. The nonlinear, second order, ordinary differential equation of motion is derived by using the fact that the system is hydrodynamically damped with external forcing. The forcing excitation is modeled as the sum of a constant current and an oscillatory wave term. Because the cables are thin and the dimension of the mass is small compared to the orbital motions of the wave particles, the fluid–structure interaction can be modeled accurately by use of the small-body theory which assumes that the presence of the structure does not influence the wave field. This implies that the waves flowing past the structure are not affected by the interaction with the structure.

The mooring angle produces a geometric nonlinearity in the restoring force that can become highly nonlinear for  $b=0$ , a two-point system, or nearly linear for  $b \gg d$  for the four-point system. The equations of motion are taken from the prototypical form for second order nonlinear differentials

$$m\ddot{X} + c\dot{X} + R(X) = F(\ddot{X}, \dot{X}, t) \quad (1)$$

where the nonlinearities are contained in the restoring force  $R(X)$  and the excitation force  $F(\ddot{X}, \dot{X}, t)$ . The restoring force describes the geometric configuration of the mooring lines and assumes linear elastic behavior so that the nonlinearity is strictly due to the geometric configuration of the system. The restoring force has the form

$$R(X) = k[X + b \operatorname{sgn}(X)]^* \left\{ 1 - \sqrt{\frac{d^2 + b^2}{d^2 + [X + b \operatorname{sgn}(X)]^2}} \right\} \quad (2)$$

and where  $\operatorname{sgn}(X)$  is the signum function defined by

$$\operatorname{sgn}(X) = \begin{cases} +1 & \text{for } X > 0 \\ 0 & \text{for } X = 0 \\ -1 & \text{for } X < 0 \end{cases} \quad (3)$$

Contributed by the Ocean Offshore and Arctic Engineering Division of ASME for publication in the JOURNAL OF OFFSHORE MECHANICS AND ARCTIC ENGINEERING. Manuscript received October 14, 2005; final manuscript received October 3, 2006. Assoc. Editor: Antonio C. Fernandes.

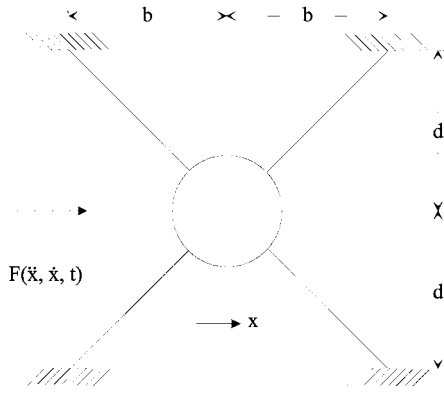


**Fig. 1 Schematic of a moored structure subject to current and wave excitation**

The excitation force is a combination of viscous drag and inertial components based upon the interactions between the moored structure and the fluid medium. This type of excitation force is found to be modeled by

$$F(\ddot{X}, \dot{X}, t) = \lambda(u - \dot{X})|u - \dot{X}| + \mu(\dot{u} - \ddot{X}) + \rho V \dot{u} \quad (4)$$

which couples the fluid motion and the structure motion through the inertial interaction between the two constituents in motion, the moored structure and the fluid medium. The system parameters are identified as the system mass  $m$ , damping  $c$ , and line stiffness  $k = 2EA / \sqrt{d^2 + b^2}$  and where  $EA$  is the elastic cable force. The line lengths  $b$  and  $d$  are observed in Fig. 1 while  $\lambda$  and  $\Phi$  are the hydrodynamic viscous drag and added mass;  $\rho$  is the fluid density; and  $V$  is the displaced volume of fluid.  $u = u(t)$  is the fluid particle velocity under current and wave excitation and is given by  $u(t) = u_0 + u_1 \sin(\omega t)$  and  $u_1 = u_1(a, \omega)$ , where  $a$  and  $\omega$  are the wave amplitude and frequency, respectively.

Assuming that the structure does not alter the fluid flow, that is, that the wave field does not change due to the motions of the moored structure, employing the small body theory, and then employing an equivalent linearization process on the quadratic drag force and finally normalizing, then, an autonomous set of first order nonlinear differential equations are obtained which are given by

$$\begin{aligned} \dot{x} &= y \\ \dot{y} &= -R(x) - \gamma y + F(x, y, \theta) \\ \dot{\theta} &= \omega \end{aligned} \quad (5)$$

where  $x = X/d$ .

Under the equivalent linearization, the nonlinearity is seen to be strictly due to the geometric configuration of the system which is manifested in the restoring force. Hence, the restoring force describes the geometric configuration of the mooring lines, assuming linear elastic behavior of the mooring lines. The restoring force has the form

$$R(x) = \Psi \left[ x + \beta \operatorname{sgn}(x) \right] \left\{ \frac{1}{\sqrt{1 + \beta^2}} - \frac{1}{\sqrt{1 + [x + \beta \operatorname{sgn}(x)]^2}} \right\} \quad (6)$$

Although the excitation force is a combination of viscous drag and inertial components based upon the interactions between the moored structure and the fluid medium, through the normalization process, the excitation force is found to have the form

$$F(x, y, \theta) = f_0 - f_1 \sin(\theta) \quad (7)$$

where the viscous drag and inertial components are combined into the current and amplitude parameters. The appropriate dimensionless constants are defined by

$$\Psi = \frac{k}{m + \mu}; \quad \beta = \frac{b}{d}; \quad \gamma = \frac{c + \lambda}{m + \mu} \quad (8)$$

The constants  $f_0$  and  $f_1$  depend upon the hydrodynamic characteristics of the system and are given by

$$f_0 = \frac{\lambda u_0}{m + \mu}; \quad f_1 = \frac{\rho V u_1}{m + \mu} \sqrt{\omega^2 (1 + C_a)^2 + \frac{1}{4} C_{dl}^2 \left( \frac{V}{S} \right)^2} \quad (9)$$

where  $C_a$  and  $C_{dl}$  are the inertial drag coefficient and the linearized drag coefficients;  $S$  is the projected drag area; and  $\rho$  is the water mass density. The associated wave frequency is obtained through the relation  $\theta = \omega t$  where  $t$  is time.

Although at first glance this system appears to be significantly more complex than the simple nonlinear systems presented in standard texts it turns out that the fluid–structure system possesses nonlinear response properties very similar to those found in classic nonlinear systems such as the Duffing system [6].

## Mooring System Response

As has been mentioned, a complete analysis of this system appears in the literature [1,2,7,8] and hence only some of the important results for the purposes of this paper are repeated. This system includes at least three types of dynamic response based upon wave and current excitation, these being periodic, quasi-periodic, and chaotic responses. A fourth state exists, when no motion is observed. This implies that the wave and current excitations are not of a significant magnitude to transfer enough energy to the mooring system in order to instigate motion. The no-motion state is uninteresting and will not be studied further. In fact, for this discussion, only the chaotic response of the system is of importance and therefore the other states will not be included.

Highly nonlinear (chaotic) oscillations are those deterministic oscillations which are characterized by a random-like, unpredictable response and yet include underlying order and structure. The unpredictability stems from the sensitivity to initial conditions. That is, two nearly identical initial conditions give rise to vastly different outcomes, they become macroscopically separated after a finite amount of time [9]. However, this alone is not enough to define sensitive (chaotic) response. A sensitive system must also possess an element of regularity as well as it must be indecomposable. The regularity usually stems from the so-called unstable periodic orbits. That is, two infinitesimally close points will come arbitrarily close to one another after a predefined period of time [4]. However, because they are unstable, the periodicity is lost under integration. The third element is the notion of indecomposability. Most easily thought of as the fact that a point within the chaotic system will enter within an arbitrarily small neighborhood of any other point at some time under the integration [9]. Putting these three conditions together, one can see that chaos poses an element of unpredictability (sensitivity to initial conditions), regularity (unstable periodic points), and the fact that it is the smallest set which contains these necessary conditions (indecomposability) [9]. Notice that these chaotic attractors are stable in the sense that as  $t \rightarrow \infty$ , all trajectories of the system tend towards them.

Figure 2 plots one of the many possible highly nonlinear (chaotic) responses of the mooring system. This example is given for the system parameter values  $\omega = 0.335$ ,  $\gamma = 0.01$ ,  $\psi = 4.0$ ,  $\beta = 0.0$ ,  $f_0 = 0.0$ , and  $f_1 = 2.0$ . Figures 2(a)–2(d) plot the: (a) Poincaré section; (b) phase space portrait; (c) frequency spectrum; and (d) a typical time series, respectively, of the chaotic response. Notice that through only small changes in the system parameters, fundamentally different response characteristics are obtained, whether it leads from periodic to chaotic dynamics or from one strange attractor to another. The presence of an abundance of these complex harmonic responses predicted by associated analytical techniques and verified by numerical results indicate that their influence on extreme and fatigue designs of the fluid–structure interaction systems may need to be considered in the future.

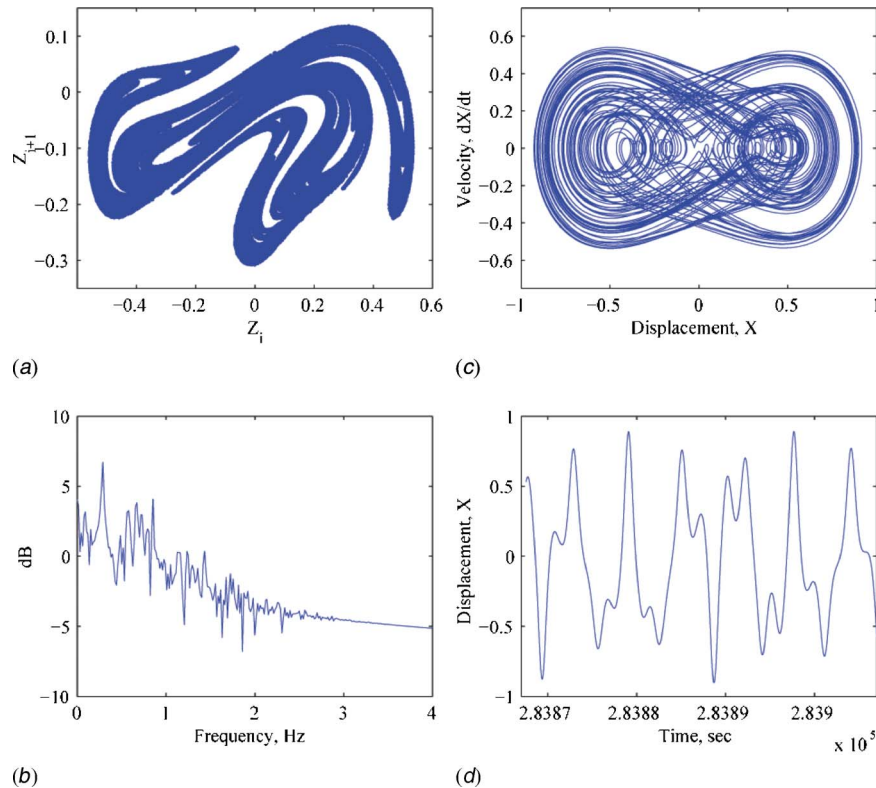


**Fig. 2** Chaotic response of the mooring system showing: (a) the Poincaré section; (b) the phase space portrait; (c) the frequency spectrum; and (d) a time series plot

### Feedback Control of Chaotic Systems

This section introduces the notion of feedback control as applied to sensitive nonlinear systems. Control of chaos has been a topic of wide research since Ott et al.[10] introduced a method, now called OGY control, in 1990. This method utilizes periodic pulses to direct a trajectory towards the stable eigenvector of a linearized model of the chaotic system.

Figure 3 is a schematic of a general feedback controller. The input is the system excitation, variables or parameters which define the system and set it into oscillation. The output is the result of the plant dynamics and any external adjustments that can be made. These external adjustments can be via control or through some random component. For now, we will consider only the purely deterministic case. The plant is a set of relations, usually differential equations, which relate the output to the input. The feedback box is a set of relations which tell how the system should be adjusted in order to maintain a certain operational state of the plant based upon known measurements.

The goal of the feedback control is to render the system dynamics into a known, stable operating mode. This can be accomplished by any of a number of methods and control theory is a rich field of study. Here, the pole placement algorithm is considered in order to place the unstable eigenvalues (poles) of the uncontrolled system within the unit circle on the complex plane, ensuring that

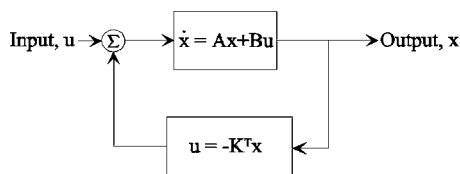


**Fig. 3** Schematic of feedback control of a general plant represented as a set of differential equations

the eigenvalues of the controlled system are stable and hence the dynamics are well behaved. This technique was devised for linear systems, however. But, because of the nature of the sensitive systems considered, there are instances under which this methodology is useful. Recall that there is a set of unstable periodic orbits embedded within any given strange attractor. These unstable periodic orbits can, in fact, be modeled by a linear set of equations and hence the linear pole placement method is applicable under these conditions.

In order to describe the nonlinear dynamics by a linear set of equations, a useful tool called Poincaré sections must be introduced. Poincaré sections are obtained by stroboscopically sampling the time series at regular intervals and then plotting one point against the previous. This has the effect of decreasing the dimension of the problem by one dimension. Moreover, it has the effect of rendering the continuous time dynamical system into a discrete time one, a feature that becomes useful for the application of control. Yet, all of the nonlinear dynamics are maintained in the reduced system. From this, the unstable periodic orbits of all orders can be identified. A linear map of a given unstable periodic orbit is constructed and this map used as the basis for the control algorithm. Because the map is unstable, it will have at least one eigenvalue greater than unity.

Once a suitable set of linear equations have been obtained, the pole placement technique can then be employed in order to render the unstable system stable [11]. Equation (10) is the feedback control law on a Poincaré section where  $Z^*$  is the centroid of the points under consideration on the Poincaré section,  $A$  is the linear map created about  $Z^*$ , and  $K^T$  is the feedback law obtained through pole placement

$$Z_{i+1} = (A - bK^T)(Z_i - Z^*) + Z^* \quad (10)$$

## Applications of Feedback Control

The algorithm to control the chaotic dynamics of the systems is to first obtain enough Poincaré points to be able to characterize an unstable periodic orbit, typically a minimum of 20 points. Once the unstable orbit is identified, a linear map is obtained by a least-squares minimization of the matrix equation involving the points near the UPO and their iterates. Given this map, a feedback law is postulated that places the control poles in a stable operating regime. Finally, the system is allowed to oscillate until the trajectory enters within  $\eta > 0$  of the UPO. At this time, control is applied to produce the desired periodic orbit.

This algorithm is successful in maintaining stable, harmonic oscillations of the mooring system under deterministic situations. The next section presents the results of the application of this control algorithm to the mooring system for primary resonance as well as a number of subharmonic resonance cases. The following section calculates a bound on the amount of energy required to achieve and maintain this control.

In the physical environment, there will be noise added to the system. Whether this noise is a random component to the excitation or strictly through measurement error, the state of the system may not be well characterized. The addition of noise is expected to present problems for the deterministic controller. The problems associated with additive noise in the mooring system are then outlined. These problems are addressed and a means to increase the controllability under the influence of a random component in the excitation is presented. Finally, the effects of the noise on the mooring system and the application of the new control methodology are presented. Estimates on the magnitude of noise under which the deterministic OGY controller is still able to function appropriately are given as well.

### The Deterministic Mooring System

In this section, the controller outlined above is applied to the mooring system. Several cases are presented to indicate the wide variety of oscillatory states that are obtainable with this method. In each case, consider the chaotic oscillations of Eqs. (5)–(7) for the parameter values given as before ( $\omega=0.335$ ,  $\gamma=0.01$ ,  $\psi=4.0$ ,  $\beta=0.0$ ,  $f_0=0.0$ , and  $f_1=2.0$ ). In order to investigate the structure of the chaotic attractor, the Poincaré section (Fig. 2(a)), the probability density of the attractor is computed to identify regions of high probability that an UPO will be found. The probability density gives a starting point for the search for UPOs and also yields a measure of the stability of the chaotic attractor under the influence of noise [11].

**Primary Resonance Control.** A search was done on the Poincaré data to obtain all points that were near a Period-1 orbit. This is done by comparing all points  $Z_i$  that are close and whose next iterate  $Z_{i+1}$  are also close (where the  $Z_i$ s are taken by stroboscopically sampling the position,  $x$ ). Then, a UPO of Period-1 is estimated as the mean of the set of points found to correspond to this set. Utilizing this method on the system structural response data, a UPO of Period-1 was found at the values  $Z^*=[x \dot{x}]^T$  where  $x=-0.2623$  and  $\dot{x}=-0.0677$ . A linear map is constructed which maps the points near the UPO  $Z^*$  toward  $Z^*$  along the direction of the stable eigenvector. In this case the linear map is given by

$$A = \begin{bmatrix} 1.4746 & -0.3997 \\ 1.4692 & -0.4450 \end{bmatrix} \quad (11)$$

which has a practically neutrally stable eigenvalue  $\lambda_u=0.9970$  and a stable eigenvalue  $\lambda_s=-0.1906$ . If the feedback control is applied only to the position  $x$ , this gives

$$b^T = [1 \ 0] \quad (12)$$

Choosing the gain vector  $K^T=[\lambda_u, -\lambda_u\lambda_s]$  yields the control poles at  $p_{1,2}=[-0.2951, 0.1044]$ . Thus, each time the system trajectory crosses the Poincaré section near  $Z^*$  the controller affects

this point by applying the control law, Eq. (10), ensuring that the trajectory returns near the point  $Z^*$  on the next return to the Poincaré section. The results of this application are shown in Fig. 4. Figure 4(a) is a plot of the Poincaré points versus time exhibiting the controlled periodic oscillation after an arbitrary duration of chaotic oscillations while Fig. 4(b) is the corresponding oscillatory state in phase space. The location on the phase space portrait where the control is applied is denoted by a circle.

The average transient length expected before being able to apply the controller is computed to be  $\langle \tau \rangle \sim 48$  iterates (returns to the Poincaré map) for the case outlined [11]. Observe that, despite the complexity of the dynamics between points in time where control is applied, the method produces a desired periodic motion through small adjustments.

**$\frac{1}{2}$  Subharmonic Control.** Again, a search was done on the Poincaré data to obtain all points that were near a Period-2 orbit. A UPO of Period-2 was found at the values  $Z^*=[x \dot{x}]^T$  where  $x=0.3301$  and  $\dot{x}=-0.1884$ . A linear map is constructed as outlined and, in this case is given by

$$A = \begin{bmatrix} 0.8793 & 0.2766 \\ 0.4553 & -0.0729 \end{bmatrix} \quad (13)$$

which has an unstable eigenvalue  $\lambda_u=1.0927$  and a stable eigenvalue  $\lambda_s=-0.0631$ . If the feedback control is applied to the position as in the previous case, and choosing the gain vector  $K^T=[\lambda_u, -\lambda_u\lambda_s]$  yields the regulator poles at  $p_{1,2}=[-0.0316 + 0.7194i, -0.0316 - 0.7194i]$ , which have magnitude 0.5186. Each time the system trajectory crosses the Poincaré section near  $Z^*$  the controller, Eq. (10) is applied ensuring that the trajectory returns near the point  $Z^*$  on the next return to the Poincaré section. The results of this simulation are shown in Fig. 4 as well. Figure 4(c) is a plot of the Poincaré points versus time and Fig. 4(d) the corresponding phase space portrait of the controlled system. Again, the location on the phase space where the control is applied is highlighted.

**$\frac{1}{3}$  Subharmonic Control.** To further demonstrate the effectiveness of this strategy, a higher order periodicity is identified and the controller is again applied, in this case a Period-3 orbit. A Period-3 orbit was identified at the point  $Z^*=[x \dot{x}]^T$  where  $x=-0.3609$  and  $\dot{x}=-0.0359$ . The linear map obtained for this case is given by

$$A = \begin{bmatrix} 0.9904 & -0.113 \\ -0.097 & -0.145 \end{bmatrix} \quad (14)$$

which has a neutrally stable and a stable eigenvalues  $\lambda_u=1.000$  and  $\lambda_s=-0.1544$ , respectively. The controller poles are placed at  $p_{1,2}=[-0.6177, 0.2068]$  and the controller is again applied to initiate control each time the system trajectory intersects the Poincaré section near the UPO at  $Z^*$  with Period-3. Figures 4(e) and 4(f) plot the results of the Period-3 control.

### Relative Energy to Maintain Control

The magnitude of the instantaneous displacement a trajectory undergoes under the action of the controller is small by construction of the algorithm, as it is for the instantaneous change in the velocity as well. Therefore, the relative energy exerted in order to maintain control with this methodology is small in comparison to the excitation force. Recall that on a given control plane, the controller is only required to be operational when a trajectory intersects a Poincaré plane and only within the ball of radius  $\eta > 0$ . The maximum distance that a trajectory can be moved on that ball is given by  $\eta/2$ , where  $\eta$  is the chosen error tolerance for the given problem (for all examples above, it was chosen as  $\eta=0.05$ ). Meanwhile, the interval of time for which control can be instigated is determined by the sampling period of the system, the control action must be completed within this interval.

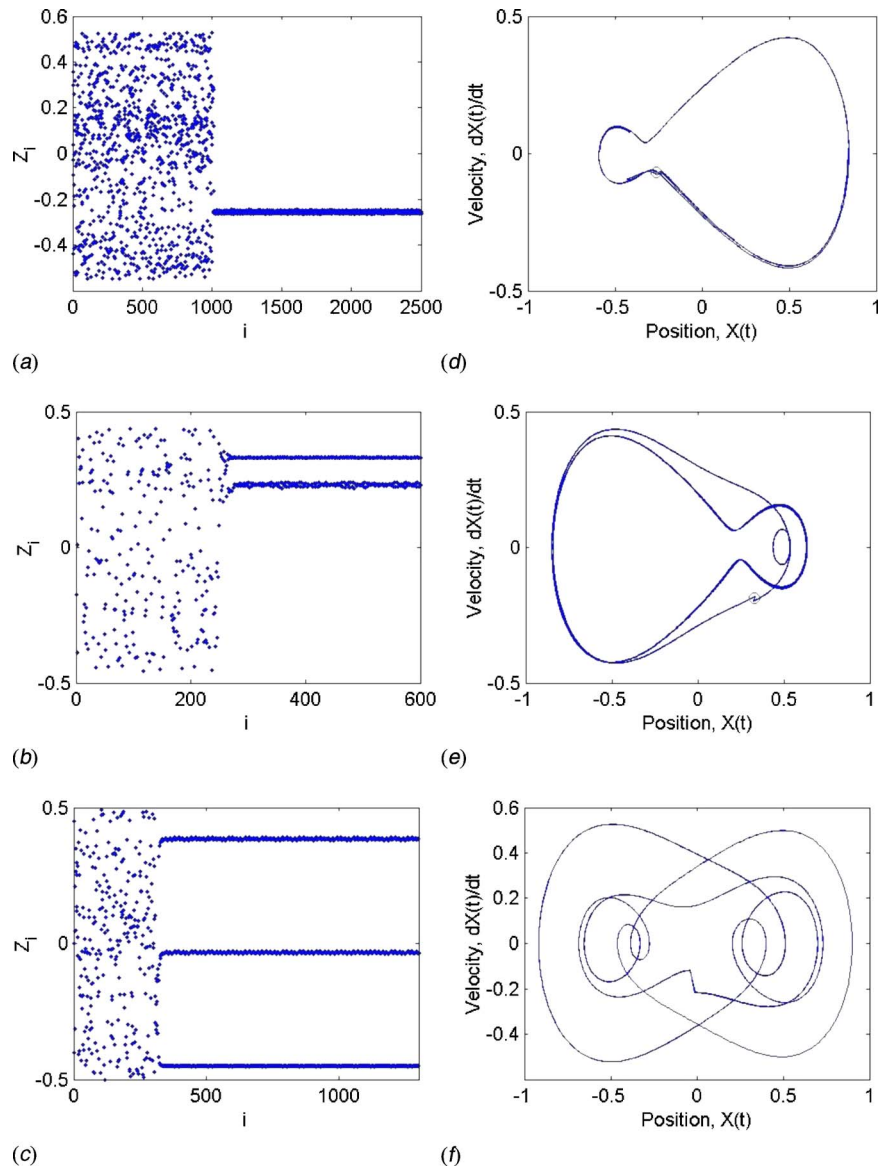


**Fig. 4 Control of the ocean mooring system (a),(b) primary resonance; (c)-(d)  $\frac{1}{2}$  subharmonic; and (e)-(f)  $\frac{1}{3}$  subharmonic**

The energy imparted to the system by the controller during a Poincaré “interval” in moving the trajectory towards the stable eigenvector from its current position is obtained through an investigation of the equilibrium equations of motion during the change in position and velocity. The (work) energy imparted to the system to change the system position is given by  $u\Delta x$ , where  $u$  is the control input and  $\Delta x$  is the change in position. Recall that the equilibrium equations can be written as

$$\ddot{x} + \gamma\dot{x} + R(x) - F(\theta) = \delta(t - T_s)u(t) \quad (15)$$

where  $\delta(t - T_s)$  indicates that  $u(t)$  is applied only on the Poincaré plane. Then, substituting the instantaneous change  $\Delta x$ , into Eq. (15) and rearranging and collecting terms the following term is obtained

$$u(T_s) = \frac{\Delta x}{\Delta t} (1 + \gamma\Delta t) + \Delta R(x) - \Delta F(\theta) \quad (16)$$

where the approximation  $\Delta\dot{x} = \Delta x / \Delta t$  is used. Here,  $\Delta x$ ,  $\Delta\dot{x}$ , and  $\Delta t$  are all known values, as well as the rest of the system param-

eters. So, the power required to instigate a movement of  $\Delta x$  is obtained by

$$P_{wr} = \left| \frac{\Delta w}{\Delta t} \right| = \left| \frac{u(T_s)\Delta x}{\Delta t} \right| \quad (17)$$

Similarly, the energy imparted to adjust the momentum is given by  $M\Delta\dot{x}^2$  where  $M = m + \mu$  for  $m$  the system mass and  $\mu$  the added mass (the mass of the displaced volume of fluid). In this case, the normalized equations of motion indicate that  $M=1$  and we have the total power required to instigate a motion in position and velocity to obtain control on a Poincaré plane as

$$P_{wr} = \left| \frac{u(T_s)\Delta x}{\Delta t} \right| + \left| \frac{\Delta\dot{x}^2}{\Delta t} \right| \quad (18)$$

For the Period-1 case, the power required to maintain instantaneous control of the system on the Poincaré plane is  $P_{wr_{\text{period-1}}} = 0.0025$  per cycle in dimensionless units. The mean power input to the system in order to instigate the nonlinear motions in the first place is give by

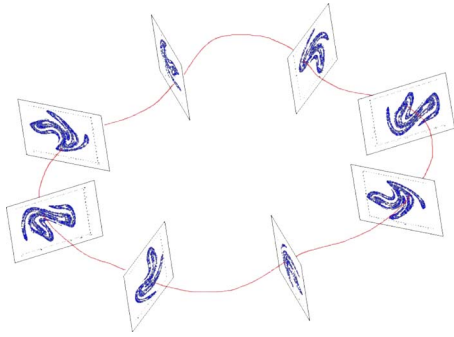


**Fig. 5 Multi-plane control is achieved by constructing  $r$  separate control planes distributed evenly throughout phase space as exhibited here for  $r=8$  for the mooring system**

$$P_{wr_{sys}} = \frac{1}{T} \int_0^T F(\theta) \frac{d\dot{x}}{dt} dt \quad (19)$$

and is calculated to be  $P_{wr_{sys}}=1.0739$  per cycle. This argument indicates that the power input required by the controller is several orders of magnitude less than the power required to drive the system, indicating that control can be achieved with little overhead to the overall design of the system.

### Effects of Additive Noise

The benefit of using small perturbations to control a deterministic nonlinear dynamical system within the chaotic operating regime has been presented above. However, for a typical, real physical system such as a moored fluid-structure system, there will be

noise added to the system through measurement errors as well as a random component in the excitation. Additive noise has the effect of destabilizing the chaotic attractor.

Here, the noise energy content is characterized by the signal-to-noise ratio (SNR) defined as  $\log_{10}(P_s/P_n)$  where  $P_s$  is the power of the noise free signal and  $P_n$  is the power of the noise and where the power is defined by

$$P = \frac{1}{T} \int_0^T x(t)^2 dt \quad (20)$$

A simple modification to the control scheme can dramatically increase the controllability of the system. A series of Poincaré sections about the chaotic attractor can be constructed by stroboscopically sampling every  $2\pi/r\Gamma$ , where  $r$  is the number of sections desired. This yields  $r$  separate controllers evenly distributed throughout the cycle as exhibited by Fig. 5, thus decreasing the long term effects of the noise with respect to an individual controller [12]. By applying the above control scheme on each Poincaré section, the UPO can be targeted from one section to the next. If these sections are selected appropriately, then the effects of the noise can be minimized.

### The Stochastic Mooring System

Figure 6 shows the Poincaré map of the noisy chaotic response obtained by adding (band limited) white noise of finite variance to the excitation term in the deterministic case as the noise intensity increases (hence the SNR decreases) from a SNR of 2.42 (Fig. 6(a)) to 1.48 (Fig. 6(d)). An examination of the corresponding probability density for this case indicates that destabilization of the sensitive dynamics manifests itself as an overall increase in the number of orbits which appear to be UPOs, but in fact are not [11].

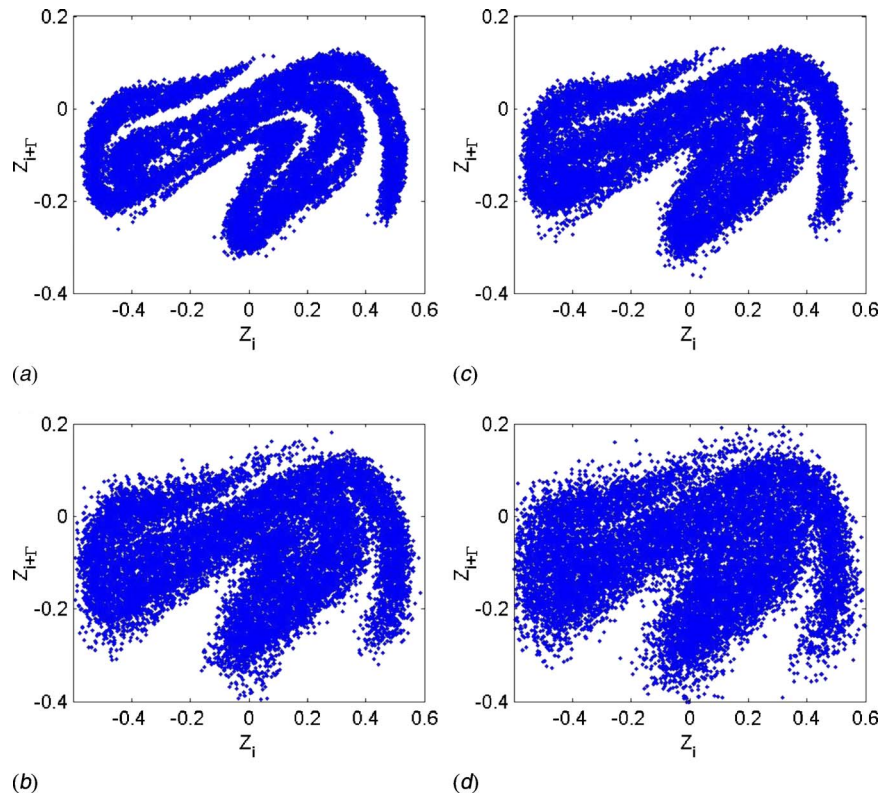


**Fig. 6 Effects of noise on the chaotic mooring system attractor as seen through the Poincaré section of the mooring system for a SNR of: (a) 2.42; (b) 2.07; (c) 1.81; and (d) 1.48**

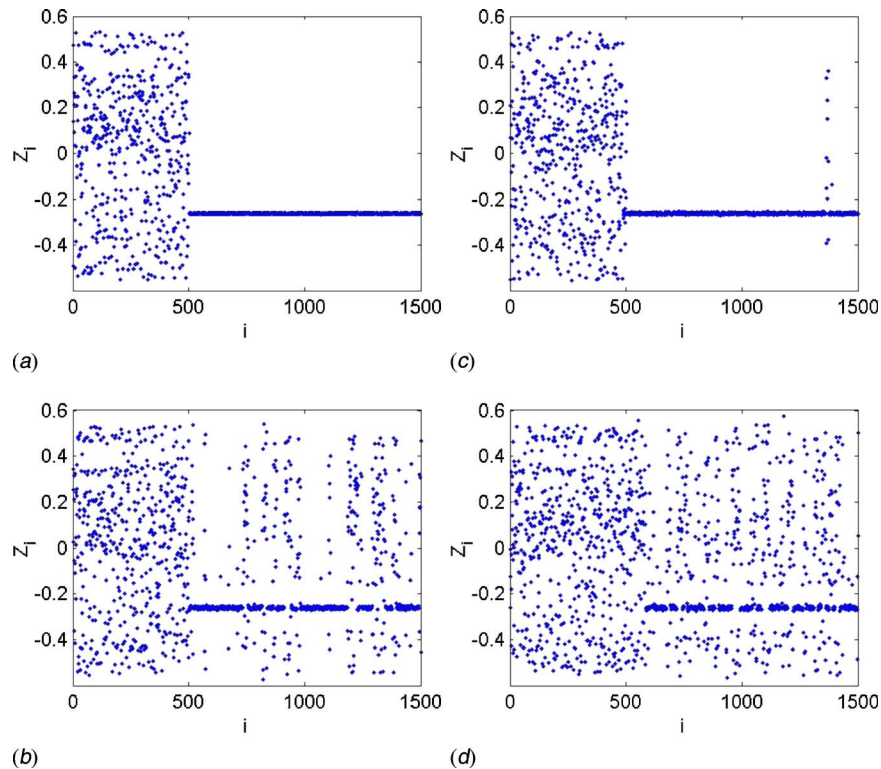


**Fig. 7 Effects of additive noise on mooring system control for the Period-1 cycle and the SNR of: (a) 2.42; (b) 2.07; (c) 1.81; and (d) 1.48**

Figure 7 plots results of the addition of the noise to the Period-1 controlled system (Figs. 4(a) and 4(b)). As the noise intensity is increased and the corresponding SNR decreases from 2.42 to 1.48 there is a corresponding destabilization of the system dynamics as well as the controller and a loss of control is realized. Observe that, as the noise level is increased, the system goes from being completely controlled, to a mode where the controller appears to be effective only for limited durations finally to the point where the effects of noise overpower the influence of the controller.

If the controller is modified to operate on multiple planes per cycle, it is expected that control will be maintained for an increasing intensity of noise. Figure 8 shows the results of the Period-1 example with noise and operating under control on eight sections, where each section has an associated linear reconstruction and controller created as outlined.

The number of control sections versus the amount of noise that the system controller is able to handle for this case is shown in Fig. 9. Here, two levels of control influence, i.e. two different values of  $\eta$  (0.05 and 0.1), are reported. It is assumed that the system is fully controlled if it can be controlled for 100 Poincaré points (or about 85,000 time series data points). This analysis indicates an approximately linear relationship between the controllable level of the energy of the noise versus the number of sections required for complete control for this system.

### Estimation and Stochastic Filtering

The previous sections introduced the idea of controlling a nonlinear, chaotic system and applied this technique to the mooring system. The control system was then tested and consequently modified in the case where additive noise is present. The extension of the control algorithm was based on the rate at which reconstructed Poincaré planes were constructed and then a linear controller was built on each of these planes. In this way, moderate amounts of noise can be handled. In order to increase the effectiveness of the control system in the presence of other than moderate levels of noise, the Kalman-Bucy filter is considered. This

section gives a brief introduction to the Kalman-bucy filter and several variants as they apply to nonlinear systems.

### The Kalman-Bucy Filter

The Kalman filter addresses the general problem of estimating the state of a first order, discrete time system that can be represented as a system of linear difference equations. (For the purposes here, it suffices to consider only the discrete time Kalman filter.) Consider the system of equations

$$x_{k+1} = Ax_k + Bu_k + w_k \quad (21)$$

with the measurement equation

$$z_k = Hx_k + v_k \quad (22)$$

where  $x_k \in \mathfrak{R}^n$  is the state variable; and  $A$  is an  $n \times n$  matrix of state coefficients relating the state at time  $k$  to the state at time  $k+1$  in the absence of either a driving force or process noise. The symbol  $u_k \in \mathfrak{R}^n$  is the vector of control inputs while  $B$  is an  $n \times l$  matrix that relates the control inputs to the state, and  $w_k$  represents the process noise. Similarly,  $z_k \in \mathfrak{R}^m$  is the measurement;  $H$  is an  $m \times n$  measurement matrix which relates the state to the measurement; and  $v_k$  is the measurement noise.

The process and measurement noise are assumed to be white noise with normal probability distributions given by

$$p(w) = N(0, Q) \quad (23)$$

$$p(v) = N(0, R) \quad (24)$$

and are assumed to be independent of one another. In practice, the noise covariance  $Q$  is either determined on some basis of intuition, or it guessed. Similarly, the measurement covariance,  $R$ , is provided by a signal processing algorithm or is again guessed. And, in general, the noise levels are determined independently, hence there are no correlations between the two noise processes. The details of the development of the Kalman filter and the iterated Kalman filter as used here can be found in King [11].

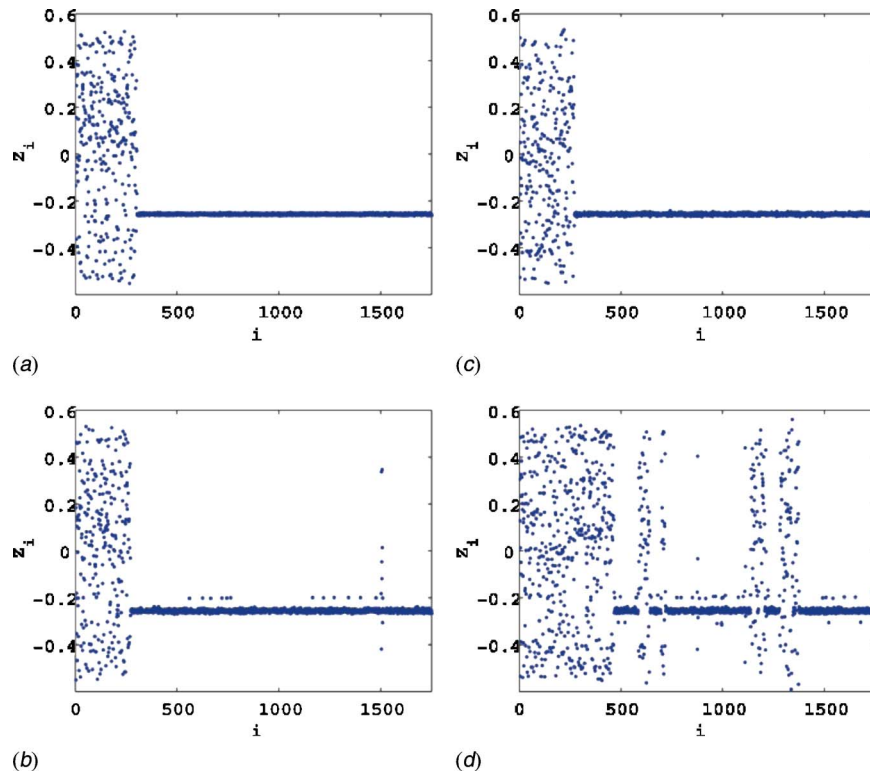


**Fig. 8 Application of the multi-plane control on the mooring system for the Period-1 case and for a SNR of: (a) 2.42; (b) 2.07; (c) 1.81; and (d) 1.48**

### Stochastic Control of Chaotic Systems

The Kalman filter data processing algorithm and its variants for nonlinear systems, the extended Kalman filter, and the iterated Kalman filter, have been successfully applied to an assortment of nonlinear and chaotic systems, both for filtering as well as control purposes [13]. The Kalman filter has also been applied in order to obtain a reference trajectory for control purposes, in this case, the extended Kalman filter was exploited [14].

For the purposes here, we apply the Kalman filter for noise reduction and then utilize the previous control method previously defined in order to bring the response of the system to a stable, periodic orbit. Of interest is the extent to which the Kalman filter can be applied under the presence of increasing noise levels while still being able to maintain system dynamics and control. That is, it is expected that the Kalman filter will successfully reduce noise levels in the systems as exhibited by the previous work, however, as the noise intensity increases, how well does the Kalman filter

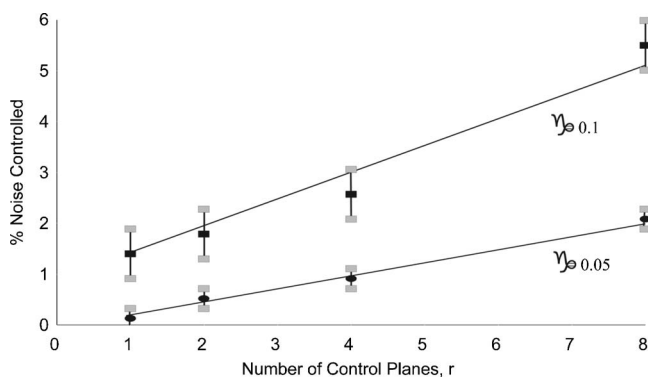


**Fig. 9 Effects of the number of control planes used versus the noise level for the mooring system**

perform? The iterated Kalman filter (IKF) is utilized since it is generally believed that the standard Kalman filter cannot successfully filter the data except under special circumstances [11]. Because of its increased potential for convergence and robustness, the IKF becomes the ideal method of ensuring stable filtering to the fiduciary trajectory, which is then used for control purposes.

Figure 10 is a diagram of the filtering and control process. The nonlinear system output at each time step is put through the Kalman filter. The estimate of the state is then used in the control algorithm to maintain stability. Recall that the system is allowed to oscillate until the trajectory enters within the  $\gamma$  ball at which time the control is applied. Also recall that this is performed on a Poincaré plane and hence, the time step indicated is that discrete time between planes. However, this can be relaxed so that the Kalman filter is applied at each numerical integration time step and the control applied only on a Poincaré plane.

Recall the nonlinear ordinary differential equations governing the evolution of the system response of the mooring system, Eqs. (5)–(7), where  $w_1(t)$  and  $w_2(t)$  are noise components added to the position and velocity, respectively. It is assumed that the frequency of excitation is known and that the noise is additive to the position and velocity alone. By “discrete mooring system,” it is

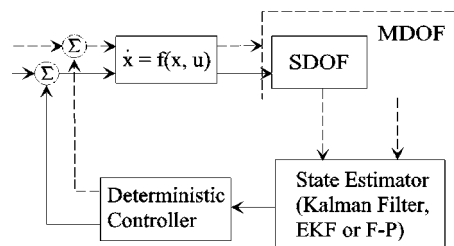


**Fig. 10 Kalman filter approach to control of the discrete time, nonlinear system**

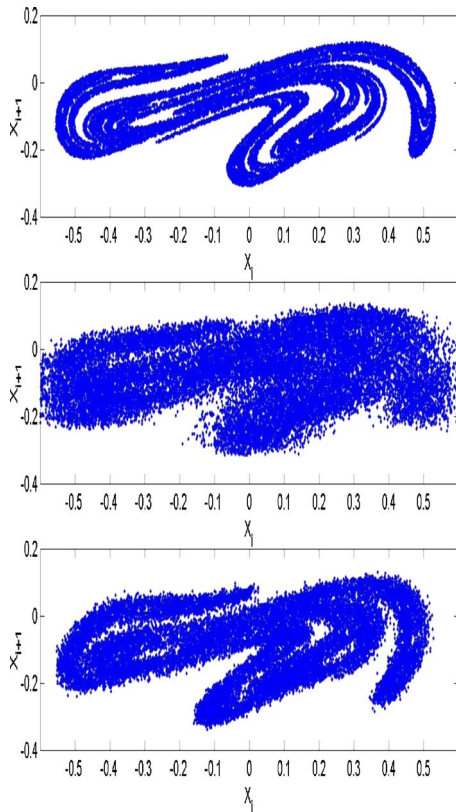


Fig. 11 Application of the IKF to the nonlinear mooring system

meant that all control actions are taken on the Poincaré plane. However, as previously indicated, the IKF is applied at each numerical integration step. Thus, the linearization procedure inherent in the IKF is applied locally at each step and the system trajectory smoothed, bringing the state back to the intended fiducial trajectory.

Using the same parameters as before, the chaotic (noise free) system response for these parameter values is seen in Figs. 2(a)–2(d). Meanwhile, the noisy chaotic response is exhibited in Fig. 8, where the Poincaré section becomes “cloudy” under the addition of noise. As is evident in Fig. 9, the addition of increased noise renders the system uncontrollable with only small amounts of noise, even as the number of control planes is increased. For this reason, the Kalman filter is applied in order to investigate the ability for the filter to reduce the effects of the noise, stochastically, for increased prediction of the current state and consequently to produce a stable, robust controller.

The implementation of the IKF introduces several parameters for which there is some control over. First, the number of Gauss–Newton iterations is predetermined. The implementation here applies a set number of iterations for the IKF update scheme as opposed to monitoring the difference between succeeding filtered points. Let  $M$  be the number of Gauss–Newton iterations. It should be apparent that if  $M=0$ , then the IKF reduces to the extended Kalman filter. The number,  $N$ , of measurement points used in the calculations can be set as well. This is the number of time measurements that will be used in the smoothing operation.

For the mooring system, the following equations define the filter inputs

$$\begin{aligned} f_1(x_1, x_2, x_3) &= x_2 \\ f_2(x_1, x_2, x_3) &= -\alpha x_1 \left( 1 - \frac{1}{\sqrt{1+x_1^2}} \right) - \gamma x_2 - f_1 \sin(x_3) \\ f_3(x_1, x_2, x_3) &= \omega \end{aligned} \quad (25)$$

where the Jacobian is given by (where  $i, j=1, 2, 3$ )

$$\frac{\partial f_i}{\partial x_j} = \begin{bmatrix} 0 & 1 & 0 \\ -\alpha \left( 1 - \frac{1}{(1+x_1^2)^{3/2}} \right) & -\gamma & -f_1 \cos(x_3) \\ 0 & 0 & 1 \end{bmatrix} \quad (26)$$

The measurement function,  $h$ , is given by

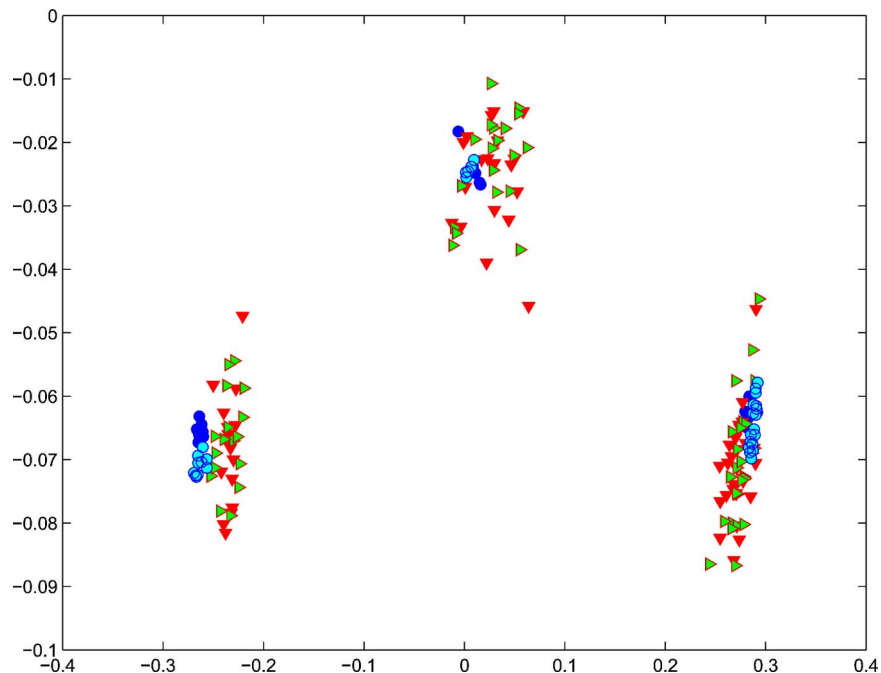


Fig. 12 Unstable periodic orbit and iterates under the influence of the IKF for three of the Period-1 cycles found within the mooring system

$$h(x) = Hx = \begin{bmatrix} 1 & 0 & 0 \\ 0 & 1 & 0 \end{bmatrix} \begin{bmatrix} x \\ y \end{bmatrix} \quad (27)$$

where, again,  $v_1(t)$  and  $v_2(t)$  are white, Gaussian, uncorrelated measurement noise variables. For the application here, it is sufficient to define the measurement functions as linear functions of the state variables. That is, we allow

$$h_1(x, y, t) = x \quad (28)$$

and

$$h_2(x, y, t) = y \quad (29)$$

so that the “linearized” measurement equations are, simply

$$\begin{bmatrix} z_1 \\ z_2 \end{bmatrix} = \begin{bmatrix} h_1(x, y, t) \\ h_2(x, y, t) \end{bmatrix} + \begin{bmatrix} v_1(t) \\ v_2(t) \end{bmatrix} \quad (30)$$

Given this representation of the state and measurement equations for the mooring system, and given the parameter values cited previously, the iterated Kalman filter can now be applied. Figure 11 is a plot of the Poincaré section for the noisy mooring system and the subsequent application of the iterated Kalman filter. Here, the noise magnitudes for the separate measurement and state noise variables are  $|w_1|=0.05$ ,  $|w_2|=0.05$ ,  $|v_1|=0.01$ ,  $|v_2|=0.01$ , and the noise magnitude for the initial conditions are 0.01, respectively. Four Gauss–Newton iterations are used while only two measurement points are utilized in the filter process. Figure 11(a) is the noiseless system response as seen on the Poincaré section while Fig. 11(b) is the noisy response. Figure 11(c) is the result of applying the iterated Kalman filter to the noisy system. Figure 12 plots three of the Period-1 orbits of the system and their iterates for the original dynamical system and the associated orbits when noise is applied and then filtered with the IKF. Here, the solid circles are the points associated with the unstable periodic orbit of the noise free system while the lightly colored circles are the iterates. The solid triangles represent the unstable periodic orbits after the filtering process and the lightly filled triangles are the iterates in this case.

Notice that the magnitude of the difference between the filtered and original dynamical system is minimized to such an extent that it is enough to achieve the desired control objective with only a single control plane, in which case, the unstable periodic orbit (the associated dynamic invariant of interest) is maintained as previously shown.

As exhibited, the iterated Kalman filter was successful in separating the noise from the chaotic signal for moderate levels of noise and consequently the control scheme previously defined is applicable. The IKF becomes a suboptimal estimator, in the least squares sense, for the nonlinear signal. This is accomplished by iterating the time update and the covariance matrix in order to obtain a more accurate estimate of the actual system trajectory shadowed. Notice, however, that the iterated Kalman filter can be used as a predictor as well.

## Concluding Remarks

This study examines control of the chaotic oscillations of a fluid–structure interaction system. The system under consideration, although of fluid origin, is modeled as a low degree of freedom system by considering cases for which the small body theory applies. The method uses a chaotic time series to categorize unstable periodic orbits. This is done by mapping the time series to a Poincaré section and then obtaining the unstable periodic

orbits through an exhaustive search of the Poincaré points. A linear map is produced for which the pole placement method of feedback control can be applied. The method was first applied to the nonlinear system to verify control. Then, the method was applied to the model in the case that band-limited white noise of finite variation was added to the excitation term, indicating that (stochastic) control of moored systems is possible. An extension of this methodology was investigated by obtaining a series of Poincaré sections, stroboscopically sampling every  $2\pi/r\Gamma$ , where  $r$  is the number of sections desired, and building a corresponding controller on each section. This yields  $r$  separate controllers evenly distributed, thus decreasing the long term effects of the noise with respect to an individual controller. Finally, under increasing levels of noise, an iterated Kalman filter was successfully applied in order to filter this noise.

Finally, should the responses of the prototypes corresponding to the model tests mentioned in the beginning of this study confirm the existence of chaotic motions in the (noisy) field environments, the analysis and control method presented in this study can be applied to suppress these motions if desired. Extensions of this study to the multi-degree-of-freedom physical models and subsequent design of practical controllers for experimental tests are being examined.

## Acknowledgment

The authors wish to acknowledge the financial support of the U.S. Bureau of Mines process control-program (Grant No. AL-92-A-001) and the United States Office of Naval Research (Grant Nos. N0001-92-J-1221 and N00014-04-10008).

## References

- [1] Gottlieb, O., and Yim, S. C. S., 1990, “Onset of Chaos in a Multi-Point Mooring System,” *Proceedings 1st (1990) European Offshore Mechanics Symposium*, Trondheim, Norway, Aug. 20–22, pp. 6–12.
- [2] Gottlieb, O., and Yim, S. C. S., 1993, “Deterministic Motions of Nonlinear Mooring Systems Part I: Analysis and Predictions,” Oregon State University, Corvallis, OR, Ocean Engineering Rep. No. OE-93-02.
- [3] Yim, S. C. S., Myrum, M. A., Gottlieb, O., Lin, H., and Shih, I. M., 1993, “Summary and Preliminary Analysis of Nonlinear Oscillations in a Submerged Mooring System Experiment,” Oregon State University, Corvallis, OR, Ocean Engineering Report No. OE-93-03.
- [4] Lathrop, D. P., and Kostelich, E. J., 1989, “Characterization of an Experimental Strange Attractor by Periodic Orbits,” *Phys. Rev. A* **40**(7), pp. 4028–4031.
- [5] Sano, M., and Sawada, Y., 1985, “Measurement of the Lyapunov Spectrum from a Chaotic Time Series,” *Phys. Rev. Lett.*, **55**(10), pp. 1082–1085.
- [6] Jordan, D. W., and Smith, P., 1999, *Nonlinear Ordinary Differential Equations*, 3rd ed., Clarendon Press, Oxford, UK.
- [7] Gottlieb, O., Feldman, M., and Yim, S. C. S., 1996, “Parameter Identification of Nonlinear Ocean Mooring Systems Using the Hilbert Transform,” *ASME J. Offshore Mech. Arct. Eng.*, **118**(1), pp. 29–36.
- [8] Gottlieb, O., Yim, S. C. S., and Lin, H., 1997, “Analysis of Bifurcation Superstructure of Nonlinear Ocean System,” *J. Eng. Mech.* **123**(11), pp. 1180–1187.
- [9] Guckenheimer, J., and Holmes, P., 1983, *Nonlinear Oscillations, Dynamical Systems, and Bifurcations of Vector Fields*, Springer, New York.
- [10] Ott, E., Grebogi, C., and Yorke, J. A., 1990, “Controlling Chaotic Dynamical Systems,” *CHAOS/XAOS, Soviet-American Perspective on Nonlinear Science*, D. Campbell, ed., American Institute of Physics, New York.
- [11] King, P. E., 2006, “Deterministic and Stochastic Control of Nonlinear Oscillations in Ocean Structural Systems,” Ph.D. dissertation, Oregon State University, Corvallis, OR.
- [12] King, P. E., and Yim, S. C. S., 1997, “Control of Noisy Chaotic Motion in a System with Nonlinear Excitation and Restoring Forces,” *Chaos*, **7**(2), pp. 290–300.
- [13] Fowler, T. B., 1989, “Application of Stochastic Control Techniques to Chaotic Nonlinear Systems,” *IEEE Trans. Autom. Control*, **34**(2), pp. 201–205.
- [14] Cazelles, B., Boudjema, G., and Chau, N. P., 1995, “Adaptive Control of Chaotic Systems in a Noisy Environment,” *Phys. Lett. A*, **196**, pp. 326–330.